Published in final edited form as:
Sci Transl Med. 2012 December 12; 4(164): 164ra159. doi:10.1126/scitranslmed.3004566.

Expression of RORγt Marks a Pathogenic Regulatory T Cell Subset in Human Colon Cancer

Nichole R. Blatner[1], **Mary F. Mulcahy**[2], **Kristen L. Dennis**[1], **Denise Scholtens**[3], **David J. Bentrem**[4,5], **Joseph D. Phillips**[4], **Soo Ham**[1], **Barry P. Sandall**[1], **Mohammad W. Khan**[1], **David M. Mahvi**[4], **Amy L. Halverson**[4], **Steven J. Stryker**[4], **Anne-Marie Boller**[4], **Ashima Singal**[1], **Rebekka K. Sneed**[1], **Bara Sarraj**[6], **Mohammed Javeed Ansari**[6], **Martin Oft**[7], **Yoichiro Iwakura**[8], **Liang Zhou**[9], **Andreas Bonertz**[10], **Philipp Beckhove**[1,10], **Fotini Gounari**[11], and **Khashayarsha Khazaie**[1,5,*]

[1]Robert H. Lurie Comprehensive Cancer Center, Northwestern University, 303 East Superior Street, Chicago, IL 60611, USA

[2]Department of Hematology/Oncology, Northwestern Medical Faculty Foundation, 676 North Saint Clair, 8th Floor, Chicago, IL 60611, USA

[3]Department of Preventive Medicine, Feinberg School of Medicine, Northwestern University, 680 North Lake Shore Drive, Suite 1400, Chicago, IL 60611, USA

[4]Department of Surgery, Feinberg School of Medicine, Northwestern University, Chicago, IL 60611, USA

[5]Jesse Brown VA Medical Center, 820 South Damen Avenue, Chicago, IL 60612, USA

[*]To whom correspondence should be addressed. khazaie@northwestern.edu.

Author contributions: N.R.B. designed and performed the experiments, analyzed the data, and wrote the paper. M.F.M. designed the experiments and provided patient samples with clinical data. D.S. performed all statistical analyses. K.L.D., J.D.P., S.H., B.P.S., and M.W.K. conducted the experiments. D.J.B., D.M.M., A.L.H., S.J.S., A.-M.B., A.S., R.K.S., B.S., M.J.A., M.O., L.Z., and Y.I. provided reagents and advice. A.B., P.B., and F.G. gave conceptual and technical advice. K.K. designed the experiments, analyzed the data, and wrote the paper.

SUPPLEMENTARY MATERIALS

www.sciencetranslationalmedicine.org/cgi/content/full/4/164/164ra159/DC1

Materials and Methods
Fig. S1. Flow cytometry gating scheme for T_{reg} fractions.
Fig. S2. Activation state of T_{reg} fractions.
Fig. S3. Example of human RORγt flow cytometry.
Fig. S4. Example of human IL-17 and IL-10 flow cytometry.
Fig. S5. Purity of human T_{regs} after FACS sorting.
Fig. S6. Cancer stage–dependent expansion of RORγt$^+$Foxp3$^+$ Fr.II T_{regs}, but not T_H17 cells, detected in the PB of CC patients.
Fig. S7. T_H17 characteristics and activation state of T_{regs}.
Fig. S8. Additional invasive polyps.
Fig. S9. Purity of mouse T_{regs} after FACS sorting and analysis of T_{reg}'s ability to suppress T cells.
Fig. S10. Cytokine and chemokine analysis of tissue lysates.
Fig. S11. Representative image of a developed ELISPOT assay.
Table S1. Patient demographics and tumor characteristics.
Table S2. Statistics for Fig. 1.
Table S3. Statistics for Fig. 2.
Table S4. Statistics for Fig. 3.
Table S5. Statistics for Fig. 4.
Table S6. Statistics for Fig. 6.
Table S7. Statistics for Fig. 7.
Table S8. Statistics for Fig. 8 and fig. S10.

Competing interests: The authors declare that they have no competing interests.

Data and materials availability: The data for this study have been deposited in the Gene Expression Omnibus database (GSE41229).

[6]Division of Nephrology and Organ Transplantation, Feinberg School of Medicine, Northwestern University, 300 East Superior Street, Chicago, IL 60611, USA

[7]Targenics Inc., 409 Illinois, Suite 5052, San Francisco, CA 94158, USA

[8]Center for Experimental Medicine and Systems Biology, Institute of Medical Science, University of Tokyo, Tokyo 108-8639, Japan

[9]Department of Microbiology-Immunology, Feinberg School of Medicine, Northwestern University, 303 East Chicago Avenue, Ward 3-120, Chicago, IL 60611, USA

[10]Division of Translational Immunology, German Cancer Research Center and National Center for Tumor Diseases, Im Neuenheimer Feld 460, 69120 Heidelberg, Germany

[11]Department of Medicine, Section of Rheumatology, University of Chicago, 5841 South Maryland Avenue, MC 0930, Chicago, IL 60637, USA

Abstract

The role of regulatory T cells (T_{regs}) in human colon cancer (CC) remains controversial: high densities of tumor-infiltrating T_{regs} can correlate with better or worse clinical outcomes depending on the study. In mouse models of cancer, T_{regs} have been reported to suppress inflammation and protect the host, suppress T cells and protect the tumor, or even have direct cancer-promoting attributes. These different effects may result from the presence of different T_{reg} subsets. We report the preferential expansion of a T_{reg} subset in human CC with potent T cell–suppressive, but compromised anti-inflammatory, properties; these cells are distinguished from T_{regs} present in healthy donors by their coexpression of Foxp3 and RORγt. T_{regs} with similar attributes were found to be expanded in mouse models of hereditary polyposis. Indeed, ablation of the RORγt gene in $Foxp3^+$ cells in polyp-prone mice stabilized T_{reg} anti-inflammatory functions, suppressed inflammation, improved polyp-specific immune surveillance, and severely attenuated polyposis. Ablation of interleukin-6 (IL-6), IL-23, IL-17, or tumor necrosis factor–α in polyp-prone mice reduced polyp number but not to the same extent as loss of RORγt. Surprisingly, loss of IL-17A had a dual effect: IL-17A–deficient mice had fewer polyps but continued to have $ROR\gamma t^+$ T_{regs} and developed invasive cancer. Thus, we conclude that RORγt has a central role in determining the balance between protective and pathogenic T_{regs} in CC and that T_{reg} subtype regulates inflammation, potency of immune surveillance, and severity of disease outcome.

INTRODUCTION

Regulatory T cells (T_{regs}), which suppress specific cytotoxic T cells (1, 2), have been shown to expand in human colon cancer (CC) and have preferential access to tumors (3). However, the contribution of T_{regs} to cancer is uncertain. T_{reg} accumulation in CC tumors has been linked with both poor (4) and favorable clinical outcomes (5-7). T_{regs} have been reported to be a good prognostic factor in gastric cancer (8), head and neck cancer (9), and breast cancer (10). Protection is speculated to be linked to the ability of T_{regs} to suppress inflammation (11-14). In addition, suppression of T helper 17 (T_H17) inflammation requires secretion of interleukin-10 (IL-10) by T_{regs} (15) and IL-10 signaling in T_{regs} and T cells (16, 17). Secretion of IL-10 by T_{regs} is also essential for suppression of Helicobacter-induced colitis (18) and gastritis (19), as well as genetically induced polyposis in mice (12).

We recently reported that T_{regs} in human CC and in mice with polyposis fail to produce IL-10 and instead produce IL-17 (14, 20). In cancer (14, 20) and in inflammatory bowel disease (21), there is detectable expression of IL-17 by T_{regs}. IL-17 and other T_H17 cytokines are elevated in the polyps and serum of mice with polyposis (14) and in human CC tumors (20), reflecting dysregulation of inflammation. Indeed, expression of IL-17 by

tumor-infiltrating lymphocytes has been negatively correlated with patient survival (5). These observations suggest that $CD4^+Foxp3^+IL\text{-}17^+$ cells are a distinct T_{reg} subset whose anti-inflammatory properties are compromised and expand in both preneoplasia and cancer.

Here, we show that IL-17–expressing T_{regs} exist within a subset of T_{regs} that express RORγt. RORγt-expressing T_{regs} expand in human CC in a cancer stage–dependentmanner and are also abundantly present in mice with polyposis. Our observations establish that expression of RORγt is linked with the inability of T_{regs} to suppress inflammation and is directly associated with the amount of inflammation and disease progression. Thus, cancer inflammation is controlled by the balance between protective T_{regs} with anti-inflammatory properties and pathogenic T_{regs} with proinflammatory properties: These T_{reg} populations are distinguished by expression of RORγt. We conclude that eliminating pathogenic T_{reg} subsets is feasible by targeting RORγt; this is a promising strategy for controlling inflammation and tumor growth in CC.

RESULTS

A distinct RORγt$^+$Foxp3$^+$ T_{reg} subset expands in human CC patients

We previously reported that $CD4^+Foxp3^+$ T cells from a small cohort of CC patients were defective in IL-10 production but produced IL-17 (20). To confirm these results, we analyzed an independent and larger population of 94 CC patients and 23 healthy donors (HDs) (table S1). To distinguish T_{regs} from $Foxp3^+$ non-T_{reg} $CD4^+$ T cells, we further sub-divided the $Foxp3^+$ lymphocytes into three different fractions as defined recently by Sakaguchi (22, 23): Fr.I $CD4^+CD45RA^+Foxp3^{int}$, Fr.II $CD4^+CD45RA^-Foxp3^{high}$, and Fr.III $CD4^+CD45RA^-Foxp3^{int}$ (Fig. 1A and fig. S1). Fr.I has naïve characteristics (CD45RA-high, CD45RO-low, CD25-int, HLADR-int), whereas Fr.II has activated characteristics (CD45RA-low, CD45RO-high, CD25-high, HLADR-high) (fig. S2). Fr.III lacks T cell–suppressive properties despite expressing Foxp3 and are, therefore, activated effector or helper T cells (22, 23). In CC, Fr.II preferentially expanded (2.9-fold) in tumors compared with healthy marginal tissue (Fig. 1B) and among peripheral blood mononuclear cells (PBMCs) of CC patients (2.5-fold) compared to PBMCs of HDs (Fig. 1, A and C). In PBMCs, there was a significant and specific increase in Fr.II with cancer stage, which was not evident in the other fractions (Fig. 1D).

Because we have previously detected elevated T_H17 cytokines in human CC tumors (20), and Fr.II and Fr.III in healthy individuals were reported to express RORC transcripts (22), we analyzed expression of the T_H17 lineage-specific transcription factor RORγt in these fractions. In CC patients, we observed enrichment of RORγt-expressing cells among Fr.II T_{regs} not only in tumor compared to marginal tissue but also among PBMCs of CC patients compared to HDs (Fig. 2A and fig. S3). A similar trend was seen for IL-17–expressing T_{regs} in tumor versus marginal tissue and in PBMCs of CC patients compared to HDs (Fig. 2B and fig. S4). However, T_{regs} expressing RORγt significantly outnumbered IL-17–expressing T_{regs} (Fig. 2C). Conversely, we observed significant decreases in expression of IL-10 by T_{regs} (Fig. 2D). Expression of IL-17 and IL-10 was mutually exclusive, except in the tumor margin where a significant population of T_{regs} expressed both cytokines (fig. S4). We previously reported that dual expression of these cytokines can indicate progression from IL-10–expressing anti-inflammatory T_{regs} to IL-17–expressing proinflammatory T_{regs} (20). To further support this notion, we FACS (fluorescence-activated cell sorting)–sorted (fig. S5) the three Foxp3-expressing fractions and tested the ability of the T_{regs} to suppressmast cell (MC) degranulation. Fr.I and Fr.II T_{regs} from CC patients were unable to suppress MC degranulation, whereas HD Fr.I and Fr.II did suppress degranulation (Fig. 3A). These observations are consistent with local as well as systemic expansion of a population of RORγt-expressing T_{regs} in human CC.

The frequency of RORγt-expressing T_{regs} in PBMCs of CC patients increased significantly from stage II to stage III (fig. S6), encouraging speculation of its value as a marker for CC progression. In contrast to RORγt-expressing T_{regs} (fig. S6A, Fr.II), we could not detect consistent cancer stage–dependent expansion of IL-17–expressing T_{regs} in CC patients (fig. S6B, Fr.II). These observations suggest that expression of RORγt in T_{regs} does not always correlate with expression of IL-17. We conclude that cancer stage–dependent T_{reg} expansion can be largely attributed to an increase in the RORγt$^+$Foxp3$^+$ subset within Fr.II.

Expression of RORγt by T_{regs} has been associated with T_{reg} plasticity, eventual loss of T_{reg}-suppressive properties, and conversion to T_H17 (24, 25). We therefore tested the ability of FACS-sorted T_{regs} from CC patients' PBMCs to suppress the proliferation of CD4 T cells. Fr.II was the most potent in suppressing the proliferation of naïve CD4 T cells in vitro, whereas Fr.III was the least effective (Fig. 3B). A similar trend was seen with T cells derived from HD PBMCs. These findings establish that the RORγt-enriched Fr.II T_{regs} of CC patients were potently T cell–suppressive and, therefore, unlikely to be in transition to T_H17 lineage commitment. To further probe this notion, we compared the cancer stage–dependent expansion of RORγt-expressing T_{regs} with expansion of T_H17-like CD4$^+$ T cells defined by their expression of RORγt or IL-17 but not Foxp3. T_H17-like T cells did not show a consistent cancer stage–dependent increase in numbers [fig. S6, compare T_H17 in (A) with T_H17 in (B)]. Therefore, expansion of the RORγt$^+$Foxp3$^+$ subset does not coincide with an increase in T_H17-like cells. Hence, our observations thus far do not support T_{reg} plasticity but indicate that the RORγt$^+$Foxp3$^+$ cells may be a stable T_{reg} subset that expands in a cancer stage–dependent manner.

Deficiency in RORγt protects against polyposis, and RORγt$^+$ T_{regs} are a major contributing factor

To evaluate the significance of expression of RORγt by T_{regs}, we resorted to the previously reported and well-characterized APC$^{\Delta 468}$ mouse model of polyposis (14, 20, 26). This mouse model contains a truncated adenomatous polyposis coli (APC) gene that leads to loss of APC function and development of benign adenomatous polyps, which are initiating events in human CC. First, we established that a significant fraction of T_{regs} in the intestine of polyp-ridden APC$^{\Delta 468}$ mice were activated and coexpressed Foxp3 and RORγt (fig. S7). As in human CC, CD4$^+$RORγt$^+$Foxp3$^+$ cells disproportionately outnumbered CD4$^+$IL-17$^+$Foxp3$^+$ cells (Fig. 4A and fig. S7A). Additionally, gene expression analysis of FACS-sorted T_{regs} revealed a T_H17 signature profile in APC$^{\Delta 468}$-derived T_{regs} compared to those from B6 mice, highlighted in T_{regs} isolated from the polyp or surrounding tissue of APC$^{\Delta 468}$ mice (Fig. 4B). Because RORγt has been suggested to be vital for T_H17 differentiation, we crossed APC$^{\Delta 468}$ mice to RORγt-deficient mice (27) to generate mice that are genetically prone to polyposis but cannot make RORγt. Surprisingly, serum levels of IL-17 in the RORγt-deficient mice were not significantly altered, although tissue IL-17 had returned to levels comparable to that found in B6 mice (Fig. 4C). Similar trends were observed for IL-1β, IL-6, and IL-23, as well as tumor necrosis factor–α (TNFα) (Fig. 4D), which have been intimately linked with a T_H17 response (14, 28-30). These findings suggest that expression of IL-17 and other T_H17 cytokines does not rely on expression of RORγt. Correlating with decreased levels of cytokines, RORγt deficiency drastically hindered polyposis in a progeny of crosses of RORγt$^{-/-}$ mice with APC$^{\Delta 468}$ mice (Fig. 5A). In contrast to unmanipulated APC$^{\Delta 468}$ mice that tend to die by 4 months of age, the RORγt-deficient counterparts survived beyond 6 months of age and still had very few polyps (Fig. 5A). Histologic analysis confirmed the benign nature of the polyps (Fig. 5, D to G).

To investigate the etiological link between RORγt, T_H17 response, and polyposis, we genetically ablated RORγt, IL-6, IL-23, IL-17, or TNFα in the bone marrow (BM) of APC$^{\Delta 468}$ mice. Polyposis was differentially affected by cytokine deficiency. Loss of IL-6 or

IL-23 caused less than a 50% reduction in polyp load, whereas loss of TNFα or IL-17 significantly attenuated polyposis (Fig. 5B). Surprisingly, and in contrast to an earlier reported protection by IL-17 deficiency (31), all $APC^{\Delta 468}$ mice with IL-17–defective BM had invasive lesions (Fig. 5, J to L, and fig. S8). Loss of RORγt in the BM of $APC^{\Delta 468}$ mice (Fig. 5B) resulted in attenuation of polyposis comparable to that found in the $ROR\gamma t^{-/-}xAPC^{\Delta 468}$ mice (Fig. 5A). Finally, to confirm that this effect was mediated by T_{regs}, we crossed Foxp3-Cre mice (32) to $ROR\gamma t^{flox/flox}$ mice, ablating the RORγt gene specifically in T_{regs}. These mice were then used as BM donors to generate BM chimeric $APC^{\Delta 468}$ mice. The resulting mice had significant attenuation of polyposis (Fig. 5C), indicating that expression of RORγt by T_{regs} is an etiological component of polyposis contributing to polyp growth.

Expression of RORγt, but not IL-17, coincides with the loss of T_{reg} anti-inflammatory function

Next, we examined the impact of RORγt deficiency versus IL-17 deficiency on expansion of proinflammatory cells during polyposis. Polyp-ridden $APC^{\Delta 468}$ mice have systemic inflammation marked by elevated numbers of proinflammatory $F4/80^{+}CD11b^{+}$ macrophages and $CD11b^{+}Gr1^{+}$ cells that include neutrophils and myeloid-derived suppressor cells (33). Loss of RORγt prevented an increase in the frequency of these cells in $APC^{\Delta 468}$ mice (Fig. 6, A and B). BM deficient for IL-17 also attenuated expansion of proinflammatory cells but less than in mice with RORγt deficiency (Fig.6, A and B). We have reported an etiological link between focal mastocytosis and polyposis in $APC^{\Delta 468}$ mice (14, 34). Furthermore, we showed earlier that T_{regs} from healthy mice potently suppress MC differentiation and function, whereas T_{regs} from polyp-ridden mice stimulate MCs (14, 20). There was a significant decrease in MC density within the polyps of RORγt-deficient mice (Fig. 6, C to F). In contrast, IL-17–deficient mice had a net increase in the density of polyp-infiltrating MCs, which was revealed by staining for MC-specific proteases (Fig. 6, C to F). There was also a qualitative difference; polyp-infiltrating MCs in $APC^{\Delta 468}$ and $ROR\gamma t^{-/-}xAPC^{\Delta 468}$ were intraepithelial and expressed mMCP2 (an MC-specific chymase) but rarely mMCP6 (an MC-specific tryptase) (Fig. 6, G and H). IL-17–deficient mice had elevated levels of MCs that expressed mMCP6, and these were located primarily in the stroma and invasive borders of the lesions (Fig. 6, G and H). These observations suggested that T_{regs} in $ROR\gamma t^{-/-}xAPC^{\Delta 468}$ mice but not in IL-17–deficient mice had recovered their anti-inflammatory properties.

To test for the anti-inflammatory properties of T_{regs}, we sorted T_{regs} from the spleen of wild-type or mutant mice at 4 months of age, confirmed their functional identity by demonstrating that they suppressed T cells in vitro and in vivo (fig. S9), and then measured their ability to suppress MC differentiation and degranulation in ex vivo assays developed by us earlier (14, 20). T_{regs} from $ROR\gamma t^{-/-}xAPC^{\Delta 468}$ mice were as suppressive as those from wild-type B6 mice, whereas T_{regs} derived from $APC^{\Delta 468}$ mice and IL-17–deficient $APC^{\Delta 468}$ mice failed to suppress MCs (Fig. 7, A and B). To validate these findings and extend them to suppression of polyposis in vivo, we adoptively transferred T_{regs} into 2.5-month-old $APC^{\Delta 468}$ mice and measured polyposis 3 weeks later, as previously described (13, 14). T_{regs} from $APC^{\Delta 468}$ mice failed to suppress polyposis, whereas T_{regs} from $ROR\gamma t^{-/-}xAPC^{\Delta 468}$ mice or from wildtype B6 mice hindered polyposis (Fig. 7C). Next, we tested the possibility that loss of RORγt rendered T_{regs} resistant to becoming proinflammatory. Although T_{regs} are potent inhibitors of MCs (35), their chronic interaction with MCs reverses this property and renders them proinflammatory (20). Upon cocultured with MCs, T_{regs} derived from wild-type B6 mice readily lost expression of IL-10 and, instead, produced IL-17, whereas $ROR\gamma t^{-/-}$ T_{regs} were completely stable, failed to produce IL-17, and maintained IL-10 expression (Fig. 7D). These observations indicate that expression of RORγt by T_{regs} is

fundamental to their phenotypic changes and subversion of their anti-inflammatory functions in polyposis.

Cancer immune surveillance is improved in RORγt-deficient APC$^{\Delta 468}$ mice

Protective antitumor T cell reactivity has been associated with a T_H17 response, raising the possibility that IL-17 or RORγt deficiencies could impair protective immunity (36, 37). Indeed, using multiplex enzyme-linked immunosorbent assay (ELISA), we found that ablation of IL-17 lowered serum levels of TH1 cytokines (Fig. 8A). However, RORγt$^{-/-}$xAPC$^{\Delta 468}$ mice had 34-fold higher levels of serum interferon-γ (IFN-γ) (Fig. 8A) and 2.5-fold higher levels in polyps (fig. S10). There were also increased serum IL-12p70 and IL-27 in the RORγt$^{-/-}$xAPC$^{\Delta 468}$ mice compared to APC$^{\Delta 468}$ mice (Fig. 8A). IFN-γ, IL-12, and IL-27 have been shown to enhance production of the chemokines IP10/CXCL10 and MIG/CXCL9, which in turn augment antitumor responses and inhibit angiogenesis (38, 39). IP10 and MIG were up-regulated in the serum and tissue lysates of RORγt$^{-/-}$xAPC$^{\Delta 468}$ mice, whereas the angiogenic factor vascular endothelial growth factor (VEGF) was diminished (Fig. 8A and fig. S10). By contrast, in the IL-17$^{-/-}$ BM-reconstituted APC$^{\Delta 468}$ mice, there was no difference in MIG, but there was a notable drop in IP10 and a significant increase in VEGF (Fig. 8A). Thus, in polyp-prone APC$^{\Delta 468}$ mice, the absence of RORγt changed the quality of the inflammatory response rather than completely abolishing it, whereas loss of IL-17 failed to suppress or improve the quality of inflammation. These findings are consistent with ablation of RORγt, causing a shift to protective immunity in APC$^{\Delta 468}$ mice.

To test for protective antitumor immunity, we measured the reactivity of T cells to polyp antigens using IFN-γ enzyme-linked immunospot (ELISPOT). Specificity of response was demonstrated by the fact that T cells from APC$^{\Delta 468}$ mice produced IFN-γ when cocultured with polyp extract–pulsed DCs, whereas similarly treated T cells from control B6 mice did not (Fig. 8B and fig. S11). Tumor-specific reactivity of T cells from RORγt$^{-/-}$xAPC$^{\Delta 468}$ mice was enhanced 1.7-fold compared to APC$^{\Delta 468}$ (Fig. 8B). By contrast, there was no significant improvement in polyp reactivity by T cells from IL-17–deficient APC$^{\Delta 468}$ mice. To further validate this finding, we performed dual immunofluorescence on paraffin-embedded sections. Coexpression of both granzyme B and perforin is necessary for efficient cell killing and tissue rejection by cytotoxic lymphocytes (40-42). Notably, the frequency of granzyme B$^+$perforin$^+$ cells infiltrating the tissue adjacent to polyps of RORγt$^{-/-}$xAPC$^{\Delta 468}$ mice was increased 6.2-fold compared to that in APC$^{\Delta 468}$ mice and 11.3-fold compared to that in IL-17–deficient APC$^{\Delta 468}$ mice (Fig. 8, C and D). There was a significant decrease in the frequency of polyp-infiltrating granzyme B$^+$perforin$^+$ cells in IL-17–deficient APC$^{\Delta 468}$ mice compared to APC$^{\Delta 468}$ mice (Fig. 8, C and D). These results demonstrate that inhibition of RORγt in polyposis primarily affects the quality of T_{regs} and does not impair, and possibly even improves, antitumor immunity.

DISCUSSION

Here, we described different T_{reg} subsets in human CC with proinflammatory and antiinflammatory phenotypes and functions. Our observations suggested that expression of RORγt marks a distinct subset of activated T_{regs} that have the potential to express IL-17. These cells expanded preferentially in CC, increased with cancer stage, and were potently T cell–suppressive. Loss of expression of IL-10 and the inability to suppress MC degranulation demonstrated that RORγt$^+$ Fr.II T_{regs} from CC patients had compromised anti-inflammatory properties. Despite the dominant T_H17 characteristic of inflammation in CC tumors (20), we did not observe a parallel increase in RORγt/IL-17–expressing CD4$^+$ T cells lacking Foxp3 expression.

Human CD4 T cells that coexpress Foxp3 and IL-17 have been observed by others (22, 43, 44). IL-17–expressing human T_{regs} expand in Crohn's disease (21) and in CC (20, 44, 45) patients. Expression of IL-17 is contingent upon activity of the transcriptional factor RORγt (46), RORα (47), or KLF4 (48). Expression of RORγt (49) or RORα (50) was considered to be incompatible with that of the key T_{reg} transcriptional factor Foxp3. Thus, T_{regs} that express RORγt together with Foxp3 were suggested to be in the transitional process of down-regulating Foxp3 and differentiating to T_H17 cells (21, 22). Our findings showed a discordance in CC between expansion of RORγt$^+$ T_{reg} and IL-17–expressing CD4 cells, suggesting that the T_{reg} subset was not differentiating to T_H17 cell.

Our observations in human CC patients were made significant by the findings that T_{regs} with similar phenotypic and functional characteristics were also present in mice that develop polyposis. Furthermore, ablating RORγt specifically in T_{regs} severely hindered polyposis. Reduction in polyp load was due to reduced inflammation and enhanced polyp-specific immunity. Loss of RORγt stabilized the anti-inflammatory properties of T_{regs}, rendering them unable to divert to a proinflammatory phenotype when cultured with MCs. On the basis of these observations, we suggest that inhibitors of RORγt may have cancer-preventive and likely therapeutic action in CC, with much of the benefits of RORγt blockade being attributed to improved T_{reg} functions and attenuation of inflammation.

It remains to be seen whether recovery of anti-inflammatory properties of T_{regs} merely reduces the level of inflammation or also improves the quality of inflammation. Importance of the quality of inflammation becomes apparent with IL-17–deficient mice. In contrast to RORγt-deficient mice, IL-17–deficient mice developed invasive cancer. T_{regs} from IL-17–deficient APC$^{\Delta 468}$ mice not only failed to suppress MC degranulation but also induced changes in the localization and protease expression of MCs that were consistent with the switch from benign to invasive cancer (51). Hence, the primary benefit of ablation of RORγt but not IL-17 is in stabilizing anti-inflammatory properties of T_{regs}.

Unexpectedly, our observations suggest that loss of IL-17 promotes cancer progression. Ablation of IL-17 in polyposisprone mice decreased the number of benign polyps but drove progression of the remaining benign intestinal lesions to become invasive carcinomas. These observations are in contrast to earlier claims that ablation of IL-17 protects against polyposis (31). Because T_H17 cells are important in host control of gut microbiota (52, 53), this discrepancy may be related to differences in the composition of gut microflora in different mouse colonies. Nevertheless, the point is made that ablation of IL-17 can produce pathogenic outcomes. In addition, IL-17 may be important for eliciting effective tumor rejection, including antitumor T cell responses (36). The potential risks of inhibiting IL-17 have not been fully investigated, and it is questionable whether this can be an effective strategy for cancer therapy.

Our findings have serious implications for immune therapy of CC. Rebalancing T_{reg} subsets rather than indiscriminate elimination of T_{regs} is likely to produce the best protection. Special consideration is needed when directly interfering with inflammation, because certain inflammatory responses such as up-regulation of IL-17 may be protective at least for progression from benign to invasive cancer. Targeting RORγt in CC may be a promising strategy for controlling expansion of proinflammatory T_{regs}, improving the quality of inflammation, and shifting from pathogenic to protective immunity.

MATERIALS AND METHODS

Patient samples

Informed consent was obtained from all participants. Institutional Review Board protocols were approved by the Scientific Review Committee of Northwestern University. All patients had histologic diagnosis of CC and had not received any previous therapy. All tumors were tested for microsatellite instability (MSI) resulting from abnormalities in DNA mismatch repair genes (MLHa, MutL, and MutS).Any MSI^+ tumor was excluded from this study. PB samples were drawn before surgical removal of the tumor.

Animals

All animal work was approved and conducted under the guidelines of Northwestern University's Animal Care and Use Committee. C57BL/6J, IL-$6^{-/-}$(B6.129S2-Il6^{tm1Kopf}/J), TNF$\alpha^{-/-}$(B6.129S-TNF^{tm1Gml}/J), Rag$^{-/-}$, RORγt^{flox}(B6-Cg-Rorc^{tm3Litt}/J), and RORγt$^{-/-}$(B6.129P2(Cg)-*Rorc*^{tm2Litt}/J) mice were purchased from Jackson Laboratories. IL-23(p19)$^{-/-}$, CD4Cre, and IL-17A$^{-/-}$ mice were previously generated by M.Oft (54), A. Rudensky (32), and Y. Iwakura (55), respectively. APC$^{\Delta 468}$ mice were previously generated by our laboratory (26).

Antibody staining and FACS

Cells were preincubated for 10 min with Fc block (BD Biosciences). For intracellular cytokine stainings, GolgiPlug (BD Biosciences), phorbol 12-myristate 13-acetate (Sigma), and ionomycin (Sigma) were added 4 hours before Fc block. Dead cells were excluded with LIVE/DEAD Violet Dead Cell Stain kit (Invitrogen). FACS acquisition was performed with a BD FACSCanto II or BD Fortessa instrument. Data analysis was conducted with FlowJo software (TreeStar). For cell sorting, DAPI was used to exclude dead cells and sorting was performed on a Dako MoFlow.

Enzyme-linked immunospot

$CD11c^+$ DCs and $CD3^+$ T cells were tested for polyp-specific reactivity on an IFN-γ ELISPOT plate (Mabtech). Data were acquired on a CTL-ImmunoSpot analyzer and analyzed with CTL ImmunoSpot software. Details are in the Supplementary Materials.

Gene expression analysis

Cells were purified from the respective organs of male Foxp3-GFP (green fluorescent protein) or Foxp3-GFPxAPC$^{\Delta 468}$ reporter mice and subjected to microarray analysis according to ImmGen standard operating procedures (http://immgen.org). Array data were normalized for background. A GenePattern Expression Dataset file was generated from genes in the T_H17 molecular signature (BioCarta). These were further analyzed with the ExpressCluster v1.3 module of the GenePattern package (Broad Institute). Replicates of each sample were grouped to calculate and cluster on the class means.

Histology

Paraffin sections (4 μm) were used throughout. Details are found in the Supplementary Materials.

Inhibition of MC progenitor differentiation

MNCs from Rag$^{-/-}$ intestine were isolated as described previously (14, 20). MNCs (10,000/100 μl) were serially diluted (1:2) in a 96-well plate containing complete medium, SCF (10 ng/ml), IL-3 (20 ng/ml), IL-2 (50 U/ml), and irradiated Rag$^{-/-}$ mouse spleen cells

(10^6/ml). T_{regs} were added 1:1. Cells were incubated for 10 to 15 days at 37°C and 5% CO_2, after which colonies of MCs were scored.

MC degranulation and inhibition by T_{regs}

MCs were presensitized with dinitrophenyl (DNP)–specific IgE (1 μg/ml), challenged in Tyrode's buffer with DNP (100 ng/ml, 30 min), and then centrifuged. Supernatants and solubilized cell pellets (0.5% Triton X-100) were incubated with *p*-nitrophenyl *N*-acetyl-β-D-glucosaminide in 0.1 M sodium citrate (pH 4.5) for 40 min at 37°C and stopped with 0.2 M glycine (pH 10.7). 4-*p*-Nitrophenol was detected by absorbance at 405 nm. Degranulation was calculated as [absorbance of the supernatant/(absorbance of supernatant + absorbance of pellet)] × 100. For T_{reg} inhibition, MCs were preincubated at 1:1 with T_{regs} for 10 min before the addition of DNP.

Serum, tissue lysates, and multiplex ELISA

Blood was collected into microcentrifuge tubes, allowed to clot, and centrifuged, and the supernatant was collected. Polyps were microdissected from the small and large bowel, minced, homogenized in 1 ml of phosphate-buffered saline, and centrifuged for 20 min at 4°C. Supernatant was filtered (0.22 μm), and protein was determined by the Bradford assay. Multiplex ELISA was conducted according to the manufacturer's instructions (Millipore). Results were acquired with a Luminex 100 instrument and analyzed with xPONENT software (Luminex Corporation).

T cell proliferation/inhibition

Sorted T cells were cultured in precoated anti-CD3 (1 μg/ml) 96-well plates for 72 hours (37°C, 5% CO_2). [^{3}H]Thymidine (1 μCi) was added, cells were incubated for 18 hours, and uptake was measured with a Perkin-Elmer MicroBeta plate counter. T_{reg} numbers were kept constant at 40,000. Non-T_{reg} CD4 cells were added at equal or increasing numbers.

Statistical analysis

Total Foxp3$^+$ and individual Fr.I, Fr.II, and Fr.III percentages were compared across HD and cancer groups with Wilcoxon rank sum tests, across tumor stage with Kruskal-Wallis tests, and between margin and tumor samples with Wilcoxon signed-rank tests for paired samples. Wilcoxon rank sum and signed-rank tests were used for all additional nonpaired and paired comparisons, respectively.

Supplementary Material

Refer to Web version on PubMed Central for supplementary material.

Acknowledgments

We thank S. Rosen for his critical comments and support and C. Benoist for his technical assistance and valuable expertise with gene expression analysis. **Funding:** Supported by the Northwestern University Interdepartmental ImmunoBiology Flow Cytometry Core Facility, The Eisenberg Foundation, Northwestern University Flow Cytometry Facility, and a Cancer Center Support Grant (National Cancer Institute CA060553); NIH grant 1R01CA160436-01, a Zell Family Award, and an anonymous foundation award of the Robert H. Lurie Comprehensive Cancer Center (to K.K.); NIH grants AI089954 and AI091962, a Pew Scholarship, and a Cancer Research Institute Investigator Award (to L.Z.); NIH grant K08AI080836-01 01 (to M.J.A.); and NIH T32 and American Society of Transplantation Basic Science Fellowship Award (to B.S.).

REFERENCES AND NOTES

1. Bonertz A, Weitz J, Pietsch DH, Rahbari NN, Schlude C, Ge Y, Juenger S, Vlodavsky I, Khazaie K, Jaeger D, Reissfelder C, Antolovic D, Aigner M, Koch M, Beckhove P. Antigen-specific Tregs control T cell responses against a limited repertoire of tumor antigens in patients with colorectal carcinoma. J Clin Invest. 2009; 119:3311–3321. [PubMed: 19809157]
2. Khazaie K, von Boehmer H. The impact of $CD4^+CD25^+$ Treg on tumor specific $CD8^+$ T cell cytotoxicity and cancer. Semin Cancer Biol. 2006; 16:124–136. [PubMed: 16443370]
3. Ling KL, Pratap SE, Bates GJ, Singh B, Mortensen NJ, George BD, Warren BF, Piris J, Roncador G, Fox SB, Banham AH, Cerundolo V. Increased frequency of regulatory T cells in peripheral blood and tumour infiltrating lymphocytes in colorectal cancer patients. Cancer Immun. 2007; 7:7. [PubMed: 17388261]
4. Sinicrope FA, Rego RL, Ansell SM, Knutson KL, Foster NR, Sargent DJ. Intraepithelial effector ($CD3^+$)/regulatory ($FoxP3^+$) T-cell ratio predicts a clinical outcome of human colon carcinoma. Gastroenterology. 2009; 137:1270–1279. [PubMed: 19577568]
5. Tosolini M, Kirilovsky A, Mlecnik B, Fredriksen T, Mauger S, Bindea G, Berger A, Bruneval P, Fridman WH, Pagès F, Galon J. Clinical impact of different classes of infiltrating T cytotoxic and helper cells (Th1, Th2, Treg, Th17) in patients with colorectal cancer. Cancer Res. 2011; 71:1263–1271. [PubMed: 21303976]
6. Correale P, Rotundo MS, Del Vecchio MT, Remondo C, Migali C, Ginanneschi C, Tsang KY, Licchetta A, Mannucci S, Loiacono L, Tassone P, Francini G, Tagliaferri P. Regulatory ($FoxP3^+$) T-cell tumor infiltration is a favorable prognostic factor in advanced colon cancer patients undergoing chemo or chemoimmunotherapy. J Immunother. 2010; 33:435–441. [PubMed: 20386463]
7. Salama P, Phillips M, Grieu F, Morris M, Zeps N, Joseph D, Platell C, Iacopetta B. Tumor-infiltrating $FOXP3^+$ T regulatory cells show strong prognostic significance in colorectal cancer. J Clin Oncol. 2009; 27:186–192. [PubMed: 19064967]
8. Haas M, Dimmler A, Hohenberger W, Grabenbauer GG, Niedobitek G, Distel LV. Stromal regulatory T-cells are associated with a favourable prognosis in gastric cancer of the cardia. BMC Gastroenterol. 2009; 9:65. [PubMed: 19732435]
9. Badoual C, Hans S, Rodriguez J, Peyrard S, Klein C, Agueznay Nel H, Mosseri V, Laccourreye O, Bruneval P, Fridman WH, Brasnu DF, Tartour E. Prognostic value of tumor-infiltrating $CD4^+$ T-cell subpopulations in head and neck cancers. Clin Cancer Res. 2006; 12:465–472. [PubMed: 16428488]
10. Ladoire S, Arnould L, Mignot G, Coudert B, Rébé C, Chalmin F, Vincent J, Bruchard M, Chauffert B, Martin F, Fumoleau P, Ghiringhelli F. Presence of Foxp3 expression in tumor cells predicts better survival in HER2-overexpressing breast cancer patients treated with neo-adjuvant chemotherapy. Breast Cancer Res Treat. 2011; 125:65–72. [PubMed: 20229175]
11. Powrie F, Read S, Mottet C, Uhlig H, Maloy K. Control of immune pathology by regulatory T cells. Novartis Found Symp. 2003; 252:92–98. [PubMed: 14609214]
12. Erdman SE, Rao VP, Poutahidis T, Ihrig MM, Ge Z, Feng Y, Tomczak M, Rogers AB, Horwitz BH, Fox JG. $CD4^+CD25^+$ regulatory lymphocytes require interleukin 10 to interrupt colon carcinogenesis in mice. Cancer Res. 2003; 63:6042–6050. [PubMed: 14522933]
13. Erdman SE, Sohn JJ, Rao VP, Nambiar PR, Ge Z, Fox JG, Schauer DB. $CD4^+CD25^+$ regulatory lymphocytes induce regression of intestinal tumors in $Apc^{Min/+}$ mice. Cancer Res. 2005; 65:3998–4004. [PubMed: 15899788]
14. Gounaris E, Blatner NR, Dennis K, Magnusson F, Gurish MF, Strom TB, Beckhove P, Gounari F, Khazaie K. T-regulatory cells shift from a protective anti-inflammatory to a cancer-promoting proinflammatory phenotype in polyposis. Cancer Res. 2009; 69:5490–5497. [PubMed: 19570783]
15. Asseman C, Mauze S, Leach MW, Coffman RL, Powrie F. An essential role for interleukin 10 in the function of regulatory T cells that inhibit intestinal inflammation. J Exp Med. 1999; 190:995–1004. [PubMed: 10510089]
16. Chaudhry A, Samstein RM, Treuting P, Liang Y, Pils MC, Heinrich JM, Jack RS, Wunderlich FT, Brüning JC, Müller W, Rudensky AY. Interleukin-10 signaling in regulatory T cells is required for

suppression of Th17 cell-mediated inflammation. Immunity. 2011; 34:566–578. [PubMed: 21511185]

17. Huber S, Gagliani N, Esplugues E, O'Connor W Jr, Huber FJ, Chaudhry A, Kamanaka M, Kobayashi Y, Booth CJ, Rudensky AY, Roncarolo MG, Battaglia M, Flavell RA. Th17 cells express interleukin-10 receptor and are controlled by $Foxp3^{-}$ and $Foxp3^{+}$ regulatory $CD4^{+}$ T cells in an interleukin-10-dependent manner. Immunity. 2011; 34:554–565. [PubMed: 21511184]
18. Tomczak MF, Erdman SE, Davidson A, Wang YY, Nambiar PR, Rogers AB, Rickman B, Luchetti D, Fox JG, Horwitz BH. Inhibition of *Helicobacter hepaticus*-induced colitis by IL-10 requires the p50/p105 subunit of NF-κB. J Immunol. 2006; 177:7332–7339. [PubMed: 17082652]
19. Lee CW, Rao VP, Rogers AB, Ge Z, Erdman SE, Whary MT, Fox JG. Wild-type and interleukin-10-deficient regulatory T cells reduce effector T-cell-mediated gastroduodenitis in $Rag2^{-/-}$ mice, but only wild-type regulatory T cells suppress *Helicobacter pylori* gastritis. Infect Immun. 2007; 75:2699–2707. [PubMed: 17353283]
20. Blatner NR, Bonertz A, Beckhove P, Cheon EC, Krantz SB, Strouch M, Weitz J, Koch M, Halverson AL, Bentrem DJ, Khazaie K. In colorectal cancer mast cells contribute to systemic regulatory T-cell dysfunction. Proc Natl Acad Sci U S A. 2010; 107:6430–6435. [PubMed: 20308560]
21. Hovhannisyan Z, Treatman J, Littman DR, Mayer L. Characterization of interleukin-17–producing regulatory T cells in inflamed intestinal mucosa from patients with inflammatory bowel diseases. Gastroenterology. 2011; 140:957–965. [PubMed: 21147109]
22. Miyara M, Yoshioka Y, Kitoh A, Shima T, Wing K, Niwa A, Parizot C, Taflin C, Heike T, Valeyre D, Mathian A, Nakahata T, Yamaguchi T, Nomura T, Ono M, Amoura Z, Gorochov G, Sakaguchi S. Functional delineation and differentiation dynamics of human $CD4^{+}$ T cells expressing the FoxP3 transcription factor. Immunity. 2009; 30:899–911. [PubMed: 19464196]
23. Sakaguchi S, Miyara M, Costantino CM, Hafler DA. $FOXP3^{+}$ regulatory T cells in the human immune system. Nat Rev Immunol. 2010; 10:490–500. [PubMed: 20559327]
24. Zhou L, Chong MM, Littman DR. Plasticity of $CD4^{+}$ T cell lineage differentiation. Immunity. 2009; 30:646–655. [PubMed: 19464987]
25. Zhou X, Bailey-Bucktrout S, Jeker LT, Bluestone JA. Plasticity of $CD4^{+}$ $FoxP3^{+}$ T cells. Curr Opin Immunol. 2009; 21:281–285. [PubMed: 19500966]
26. Gounari F, Chang R, Cowan J, Guo Z, Dose M, Gounaris E, Khazaie K. Loss of adenomatous polyposis coli gene function disrupts thymic development. Nat Immunol. 2005; 6:800–809. [PubMed: 16025118]
27. Eberl G, Marmon S, Sunshine MJ, Rennert PD, Choi Y, Littman DR. An essential function for the nuclear receptor RORγt in the generation of fetal lymphoid tissue inducer cells. Nat Immunol. 2004; 5:64–73. [PubMed: 14691482]
28. Charles KA, Kulbe H, Soper R, Escorcio-Correia M, Lawrence T, Schultheis A, Chakravarty P, Thompson RG, Kollias G, Smyth JF, Balkwill FR, Hagemann T. The tumor-promoting actions of TNF-α involve TNFR1 and IL-17 in ovarian cancer in mice and humans. J Clin Invest. 2009; 119:3011–3023. [PubMed: 19741298]
29. Takahashi N, Vanlaere I, de Rycke R, Cauwels A, Joosten LA, Lubberts E, van den Berg WB, Libert C. IL-17 produced by Paneth cells drives TNF-induced shock. J Exp Med. 2008; 205:1755–1761. [PubMed: 18663129]
30. Sugita S, Kawazoe Y, Imai A, Yamada Y, Horie S, Mochizuki M. Inhibition of Th17 differentiation by anti-TNF-alpha therapy in uveitis patients with Behçet's disease. Arthritis Res Ther. 2012; 14:R99. [PubMed: 22546542]
31. Chae WJ, Gibson TF, Zelterman D, Hao L, Henegariu O, Bothwell AL. Ablation of IL-17A abrogates progression of spontaneous intestinal tumorigenesis. Proc Natl Acad Sci U S A. 2010; 107:5540–5544. [PubMed: 20212110]
32. Rubtsov YP, Rasmussen JP, Chi EY, Fontenot J, Castelli L, Ye X, Treuting P, Siewe L, Roers A, Henderson WR Jr, Muller W, Rudensky AY. Regulatory T cell-derived interleukin-10 limits inflammation at environmental interfaces. Immunity. 2008; 28:546–558. [PubMed: 18387831]

33. Gounaris E, Tung CH, Restaino C, Maehr R, Kohler R, Joyce JA, Ploegh HL, Barrett TA, Weissleder R, Khazaie K. Live imaging of cysteine-cathepsin activity reveals dynamics of focal inflammation, angiogenesis, and polyp growth. PLoS One. 2008; 3:e2916. [PubMed: 18698347]
34. Gounaris E, Erdman SE, Restaino C, Gurish MF, Friend DS, Gounari F, Lee DM, Zhang G, Glickman JN, Shin K, Rao VP, Poutahidis T, Weissleder R, McNagny KM, Khazaie K. Mast cells are an essential hematopoietic component for polyp development. Proc Natl Acad Sci U S A. 2007; 104:19977–19982. [PubMed: 18077429]
35. Piconese S, Gri G, Tripodo C, Musio S, Gorzanelli A, Frossi B, Pedotti R, Pucillo CE, Colombo MP. Mast cells counteract regulatory T-cell suppression through interleukin-6 and OX40/OX40L axis toward Th17-cell differentiation. Blood. 2009; 114:2639–2648. [PubMed: 19643985]
36. Ma Y, Aymeric L, Locher C, Mattarollo SR, Delahaye NF, Pereira P, Boucontet L, Apetoh L, Ghiringhelli F, Casares N, Lasarte JJ, Matsuzaki G, Ikuta K, Ryffel B, Benlagha K, Tesnière A, Ibrahim N, Déchanet-Merville J, Chaput N, Smyth MJ, Kroemer G, Zitvogel L. Contribution of IL-17–producing γδ T cells to the efficacy of anticancer chemotherapy. J Exp Med. 2011; 208:491–503. [PubMed: 21383056]
37. Martin-Orozco N, Muranski P, Chung Y, Yang XO, Yamazaki T, Lu S, Hwu P, Restifo NP, Overwijk WW, Dong C. T helper 17 cells promote cytotoxic T cell activation in tumor immunity. Immunity. 2009; 31:787–798. [PubMed: 19879162]
38. Engel MA, Neurath MF. Anticancer properties of the IL-12 family—Focus on colorectal cancer. Curr Med Chem. 2010; 17:3303–3308. [PubMed: 20712574]
39. Xu M, Mizoguchi I, Morishima N, Chiba Y, Mizuguchi J, Yoshimoto T. Regulation of antitumor immune responses by the IL-12 family cytokines, IL-12, IL-23, and IL-27. Clin Dev Immunol. 2010; 2010:832454. [PubMed: 20885915]
40. Rousalova I, Krepela E. Granzyme B-induced apoptosis in cancer cells and its regulation (review). Int J Oncol. 2010; 37:1361–1378. [PubMed: 21042704]
41. Baran K, Dunstone M, Chia J, Ciccone A, Browne KA, Clarke CJ, Lukoyanova N, Saibil H, Whisstock JC, Voskoboinik I, Trapani JA. The molecular basis for perforin oligomerization and transmembrane pore assembly. Immunity. 2009; 30:684–695. [PubMed: 19446473]
42. Boivin WA, Cooper DM, Hiebert PR, Granville DJ. Intracellular versus extracellular granzyme B in immunity and disease: Challenging the dogma. Lab Invest. 2009; 89:1195–1220. [PubMed: 19770840]
43. Beriou G, Costantino CM, Ashley CW, Yang L, Kuchroo VK, Baecher-Allan C, Hafler DA. IL-17–producing human peripheral regulatory T cells retain suppressive function. Blood. 2009; 113:4240–4249. [PubMed: 19171879]
44. Kryczek I, Wu K, Zhao E, Wei S, Vatan L, Szeliga W, Huang E, Greenson J, Chang A, Roliński J, Radwan P, Fang J, Wang G, Zou W. IL-17^{+} regulatory T cells in the microenvironments of chronic inflammation and cancer. J Immunol. 2011; 186:4388–4395. [PubMed: 21357259]
45. Wilke CM, Kryczek I, Wei S, Zhao E, Wu K, Wang G, Zou W. Th17 cells in cancer: Help or hindrance? Carcinogenesis. 2011; 32:643–649. [PubMed: 21304053]
46. Ivanov II, McKenzie BS, Zhou L, Tadokoro CE, Lepelley A, Lafaille JJ, Cua DJ, Littman DR. The orphan nuclear receptor RORγt directs the differentiation program of proinflammatory IL-17^{+} T helper cells. Cell. 2006; 126:1121–1133. [PubMed: 16990136]
47. Yang XO, Pappu BP, Nurieva R, Akimzhanov A, Kang HS, Chung Y, Ma L, Shah B, Panopoulos AD, Schluns KS, Watowich SS, Tian Q, Jetten AM, Dong C. T helper 17 lineage differentiation is programmed by orphan nuclear receptors RORα and RORγ. Immunity. 2008; 28:29–39. [PubMed: 18164222]
48. Lebson L, Gocke A, Rosenzweig J, Alder J, Civin C, Calabresi PA, Whartenby KA. Cutting edge: The transcription factor Kruppel-like factor 4 regulates the differentiation of Th17 cells independently of RORγt. J Immunol. 2010; 185:7161–7164. [PubMed: 21076063]
49. Zhou L, Lopes JE, Chong MM, Ivanov II, Min R, Victora GD, Shen Y, Du J, Rubtsov YP, Rudensky AY, Ziegler SF, Littman DR. TGF-β-induced Foxp3 inhibits T_H17 cell differentiation by antagonizing RORγt function. Nature. 2008; 453:236–240. [PubMed: 18368049]
50. Du J, Huang C, Zhou B, Ziegler SF. Isoform-specific inhibition of RORα-mediated transcriptional activation by human FOXP3. J Immunol. 2008; 180:4785–4792. [PubMed: 18354202]

51. Khazaie K, Blatner NR, Khan MW, Gounari F, Gounaris E, Dennis K, Bonertz A, Tsai FN, Strouch MJ, Cheon E, Phillips JD, Beckhove P, Bentrem DJ. The significant role of mast cells in cancer. Cancer Metastasis Rev. 2011; 30:45–60. [PubMed: 21287360]

52. Ivanov II, Littman DR. Segmented filamentous bacteria take the stage. Mucosal Immunol. 2010; 3:209–212. [PubMed: 20147894]

53. Korn T, Bettelli E, Oukka M, Kuchroo VK. IL-17 and Th17 cells. Annu Rev Immunol. 2009; 27:485–517. [PubMed: 19132915]

54. Langowski JL, Zhang X, Wu L, Mattson JD, Chen T, Smith K, Basham B, McClanahan T, Kastelein RA, Oft M. IL-23 promotes tumour incidence and growth. Nature. 2006; 442:461–465. [PubMed: 16688182]

55. Nakae S, Komiyama Y, Nambu A, Sudo K, Iwase M, Homma I, Sekikawa K, Asano M, Iwakura Y. Antigen-specific T cell sensitization is impaired in IL-17-deficient mice, causing suppression of allergic cellular and humoral responses. Immunity. 2002; 17:375–387. [PubMed: 12354389]

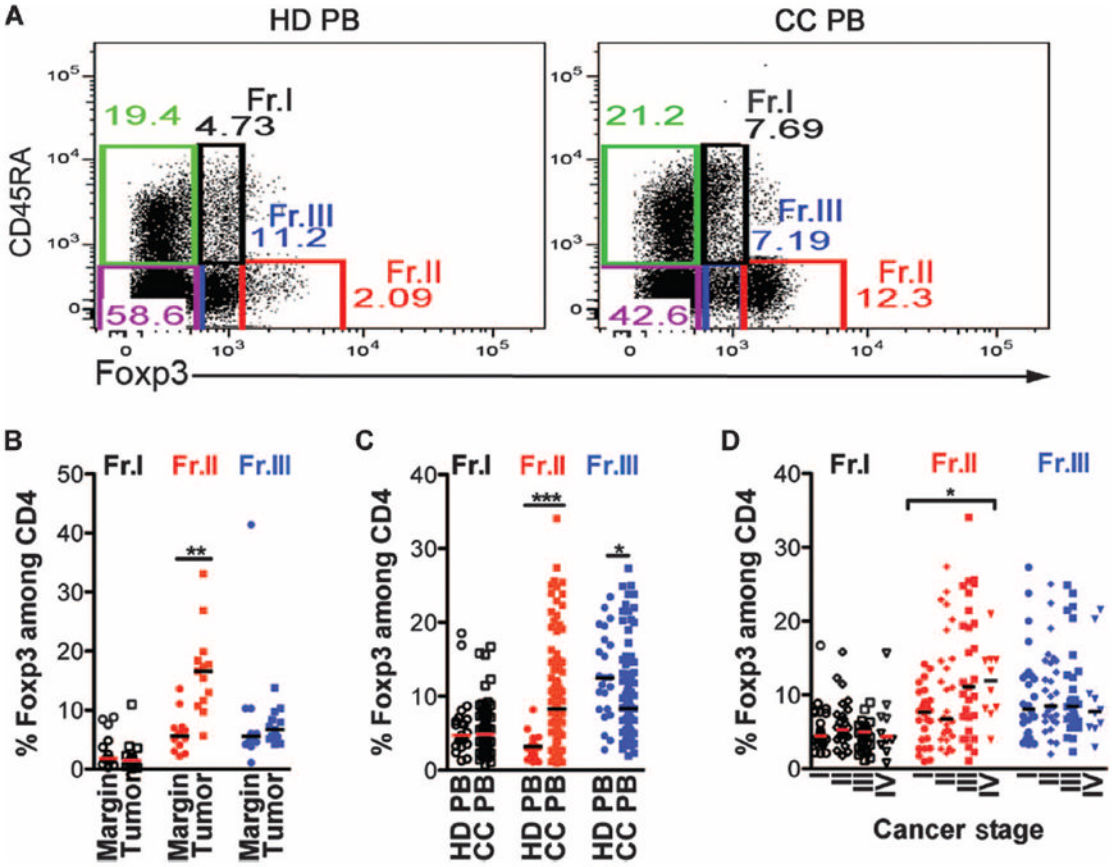

Fig. 1.

In human CC, Fr.II T_{regs} expand in a cancer stage–dependent manner. (**A**) Representative dot plots depicting flow cytometry gating of five T cell fractions: three of which are $Foxp3^+$ and two are $Foxp3^-$. The $Foxp3^+$ cells are labeled as Fr.I (black, $CD45RA^+Foxp3^{int}$), Fr.II (red, $CD45RA^-Foxp3^{high}$), and Fr.III (blue, $CD45RA^-Foxp3^{int}$). Non-Foxp3 T cells can be divided into naïve $CD45RA^+Foxp3^-$ (green) and memory $CD45RA^-Foxp3^-$ (purple). Cells were pregated on live $CD4^+CD8^-$ cells. (**B**) Compiled frequencies of T_{reg} subtypes among CD4 T cells frommarginal or tumor tissue as determined by FACS analysis ($n = 13$). (**C**) Compiled frequencies of T_{reg} subtypes among CD4 T cells from PBMCs of HD or CC patients. HD, $n = 23$; CC, $n = 94$. (**D**) CC PBMC T_{reg} subtype frequencies according to the cancer stage of each CC patient as defined by the International Union for Cancer Control. Fr.I: white circles, HD; white squares, CC; Fr.II: red circles, HD; red squares, CC; Fr.III: blue circles, HD; blue squares, CC. Statistics are found in table S2. Bar represents median. Each dot in (B) to (D) represents one patient; value was determined from an average of at least two separate FACS stainings.

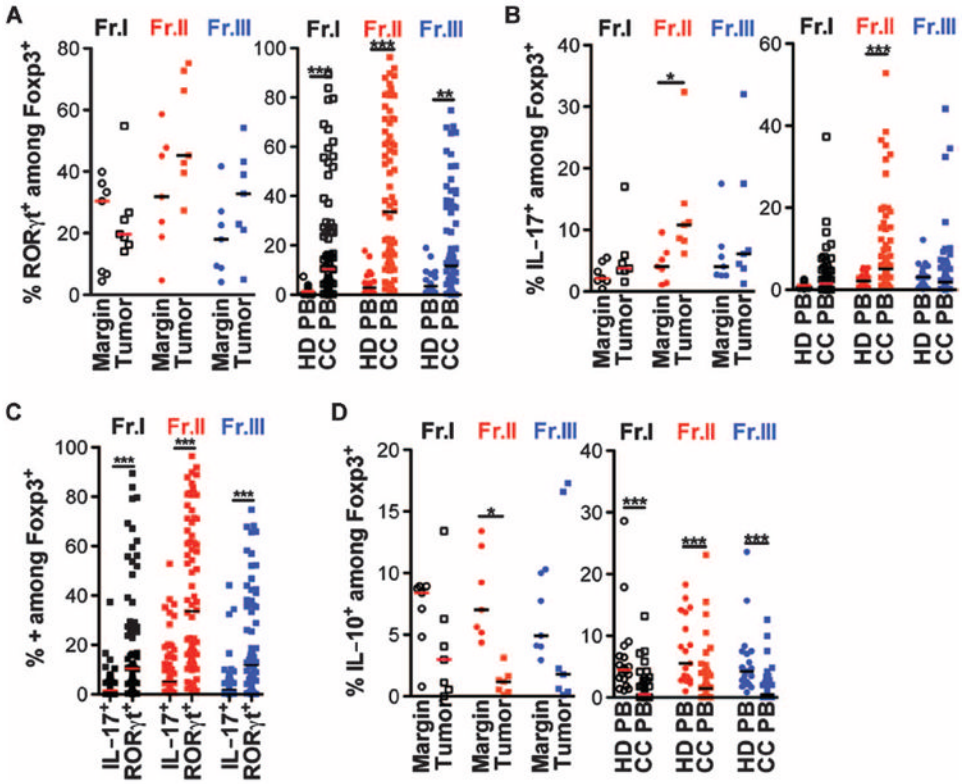

Fig. 2.

CC Fr.II T_{regs} express a high frequency of RORγt and a minimal amount of anti-inflammatory IL-10. (**A**) Compiled frequencies of RORγt expression among each $Foxp3^+$ fraction isolated from CC tissue (left panel, $n = 7$) or PBMCs of HD or CC PB (right panel, $n = 21$ and 74, respectively). (**B**) Compiled frequencies of IL-17 expression among each $Foxp3^+$ fraction isolated from CC tissue (left panel, $n = 6$) or PBMCs of HD or CC PB (right panel, $n = 21$ and 71, respectively). (**C**) Side-by-side comparison of the frequency of IL-17– or RORγt-expressing $Foxp3^+$ within each fraction from CC PBMCs. Black squares, Fr.I; red squares, Fr.II; blue squares, Fr.III. (**D**) Compiled frequencies of IL-10 expression among each $Foxp3^+$ fraction isolated from CC tissue (left panel, $n = 6$) or PBMCs of HD or CC PB (right panel, $n = 19$ and 69, respectively). For (A), (B), and (D): Fr.I: white circles, HD; white squares, CC; Fr.II: red circles, HD; red squares, CC; Fr.III: blue circles, HD; blue squares, CC. Statistics are found in table S3. Bar represents median.

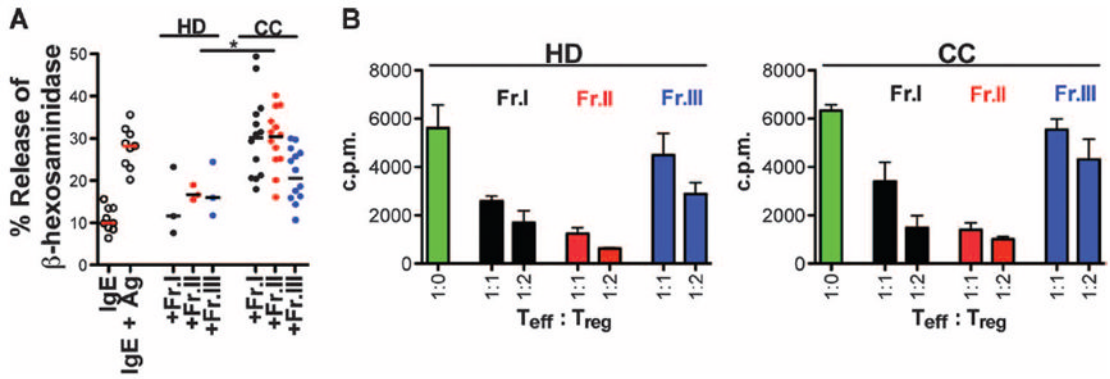

Fig. 3.

CC Fr.II T_{regs} are potently T cell–suppressive but lack the ability to suppress MC degranulation. (**A**) Compiled values of percent LAD2-MC degranulation sensitized with immunoglobulin E (IgE), cross-linked with anti-IgE + antigen (Ag), or incubated with FACS-sorted T_{reg} population isolated from HD ($n = 3$) or CC ($n = 14$) PBMCs. Bar represents median. Statistics are found in table S4. (**B**) Both Fr.I (black) and Fr.II (red) T_{regs} from PBMCs of HD (left panel, $n = 2$) or CC (right panel, $n = 3$) suppress the proliferation of naïve $CD45RA^{+}CD4^{+}CD25^{-}Foxp3^{-}$ T cells (green); Fr.III T_{regs} (blue) do not suppress T cell proliferation. T_{eff}, effector T cells. Each tested in duplicate. Mean and SEM are depicted.

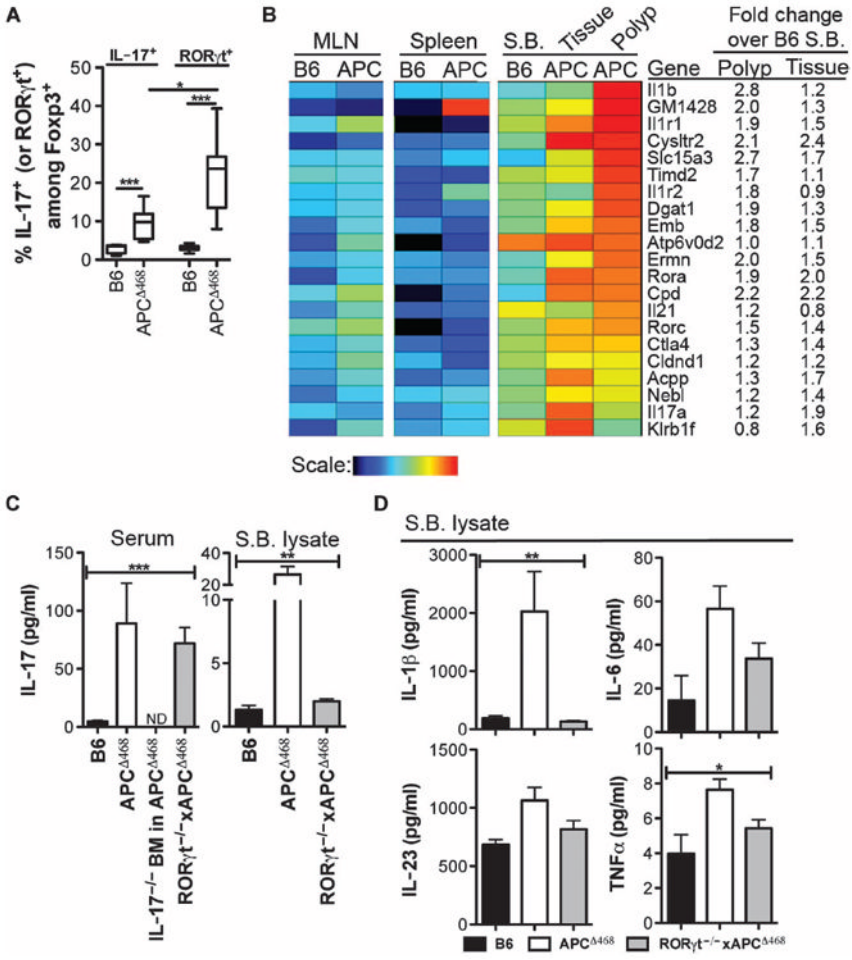

Fig. 4.

Loss of RORγt prevents excessive T_H17 response but does not abolish it. (**A**) Frequency of IL-17$^+$ or RORγt$^+$ cells among Foxp3$^+$ cells. Comparing APC$^{\Delta 468}$ IL-17$^+$Foxp3$^+$ to APC$^{\Delta 468}$ RORγt$^+$Foxp3$^+$, $P = 0.0111$. (**B**) Heat map of ExpressCluster v1.3 showing the expression of components of the T_H17 molecular signature in T_{regs} isolated from the indicated tissues and mice ($n = 3$). (**C**) Expression of IL-17 protein in the serum and small bowel (S.B.) lysate as determined by multiplex ELISA. (**D**) Additional T_H17-associated cytokines were also detected with multiplex ELISA from small bowel lysate. Mean and SEM are depicted. Sera from five mice were each tested in duplicate. Lysates from polyps of threemice were each tested in duplicate. Statistics are found in table S5.

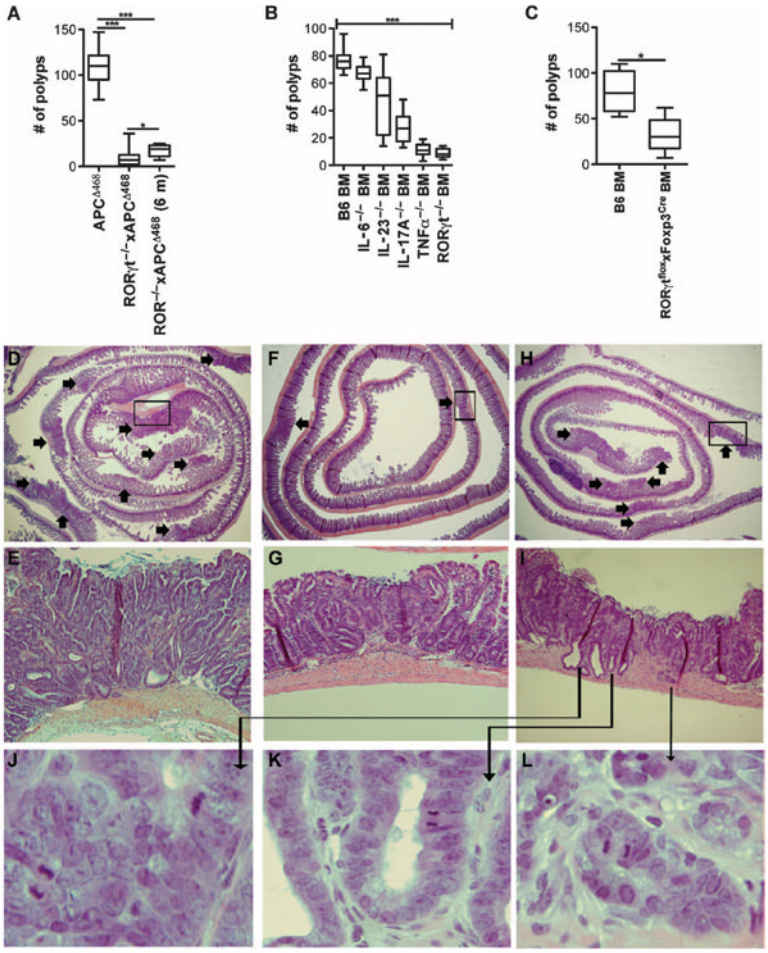

Fig. 5.

Loss of T_H17 cytokines reduces polyp number, but loss of IL-17 promotes invasion. (**A**) $APC^{\Delta 468}$ mice were crossed to $ROR\gamma t^{-/-}$, and polyp load was determined at 4 or 6 months of age: $APC^{\Delta 468}$ = 109 ± 19, n = 25; $ROR\gamma t^{-/-}xAPC^{\Delta 468}$ (4 m) = 9 ± 9, $P < 0.0001$, n = 22; $ROR\gamma t^{-/-}xAPC^{\Delta 468}$ (6 m) = 18 ± 7, $P < 0.001$, n = 7; comparing $ROR\gamma t^{-/-}xAPC^{\Delta 468}$ 4 m to 6 m, P = 0.0152; mean ± SD, P value determined by Wilcoxon rank sum test. (**B**) $APC^{\Delta 468}$ mice were lethally irradiated at 6 weeks of age, reconstituted with BM progenitor cells from control B6 BM or BM deficient in IL-6, IL-23, IL-17A, TNFα, or RORγt, and allowed to age to 4 months of age. The number of polyps was then counted: B6 = 76 ± 3, n = 10; IL-$6^{-/-}$ = 67 ± 2, n = 10; IL-$23^{-/-}$ = 45 ± 6, n = 15; IL-$17A^{-/-}$ = 27 ± 4, n = 9; $ROR\gamma t^{-/-}$ = 8 ± 2, n = 5; $P < 0.0001$ using Kruskal-Wallis test comparing all. (**C**) $APC^{\Delta 468}$ mice were reconstituted at 6 weeks of age with control B6 BM or BM derived from $ROR\gamma t^{flox}xFoxp3^{Cre}$ mice and allowed to age to 4 months of age. The number of polyps was then counted: B6 BM = 80 ± 24, n = 4; $ROR\gamma t^{flox}xFoxp3^{Cre}$ BM = 32 ± 20, n = 5; P = 0.032 determined by Wilcoxon rank sum test. (**D** to **L**) Representative hematoxylin and eosin of “jelly-roll” paraffin-embedded sections from 4-month-old mice: (D and E) $APC^{\Delta 468}$, (F and G) $ROR\gamma t^{-/-}xAPC^{\Delta 468}$, and (H to L) IL-$17^{-/-}$ BM in $APC^{\Delta 468}$. Arrows indicate polyps. (E, G, and I) ×200 Magnification of the boxed area in the panel above. (J to L) ×400 Magnification of invasive polyps depicted in (I).

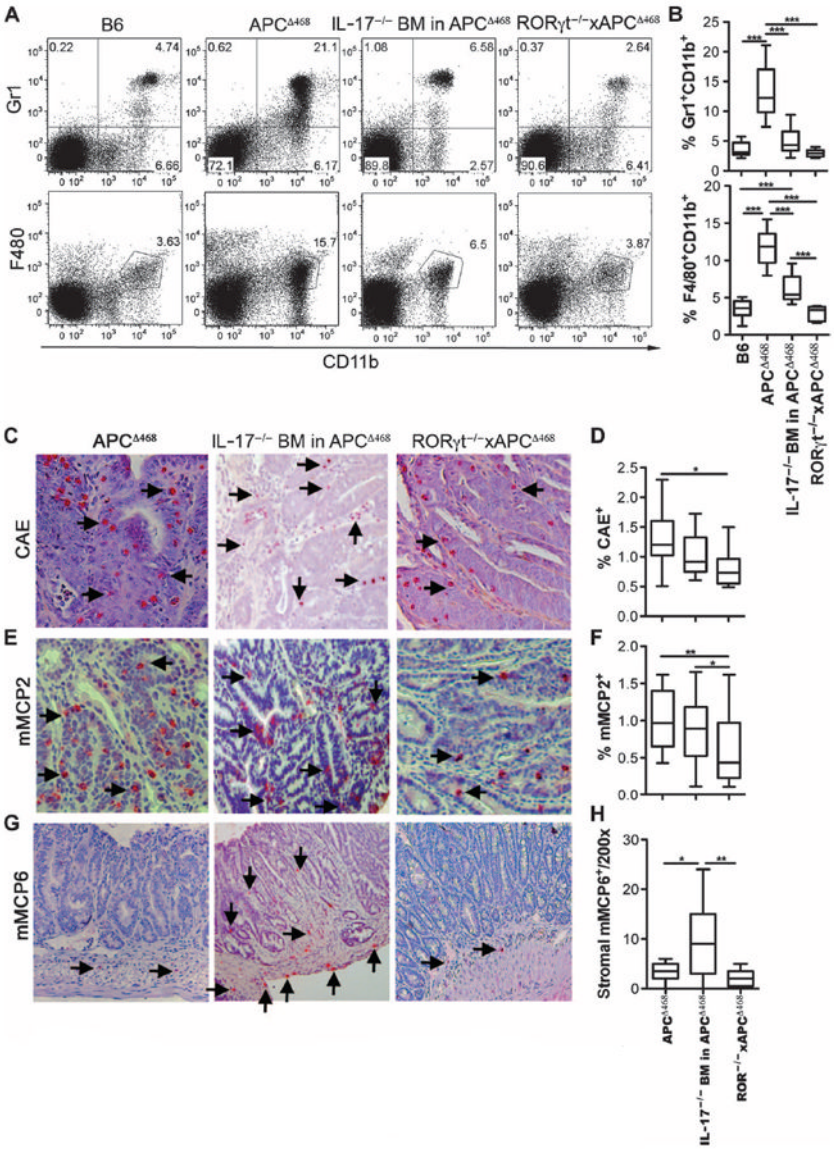

Fig. 6.

Loss of RORgγt or IL-17 in polyp-pronemice differentially affects systemic and local inflammation. (**A**) Representative dot plots of $Gr1^+CD11b^+$ (top panel) and $F4/80^+CD11b^+$ (bottom panel) cells in the spleens of 4-month-oldmice. Cells are pregated for live cells. (**B**) Compiled frequencies of $Gr1^+CD11b^+$ (top) and $F4/80^+CD11b^+$ (bottom) cells. (**C** to **H**) Immunohistochemistry of paraffin sections from $APC^{\Delta 468}$ (left columns), IL-$17^{-/-}$ BM in $APC^{\Delta 468}$ (middle columns), and RORγ$t^{-/-}$x$APC^{\Delta 468}$ (right columns) mice stained with chloroacetate esterase (CAE) (C), mMCP2 (E), or mMCP6 (G). Arrows point to stained cells. Frequency of polyp-infiltrating (D) CAE-positive or (F) mMCP2-positive cells among total cells within a 200× field of view. (H) Total number of mMCP6-positive cells found within the stroma of a polyp within a 200× field of view. For all graphs, bar represents median. Statistics are found in table S6.

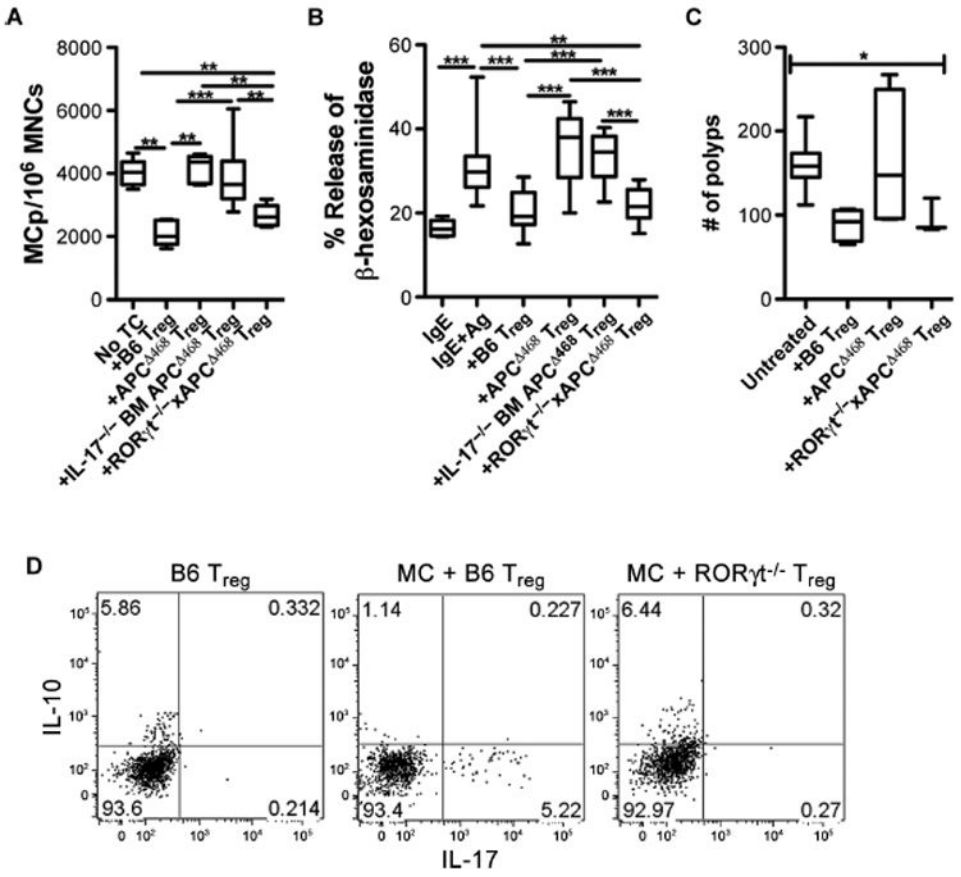

Fig. 7.

Loss of RORγt, but not IL-17, restores T_{reg} anti-inflammatory function. (**A**) Frequency of MC progenitors (MCp) among total mononuclear cells (MNCs) isolated from the intestine of $Rag^{-/-}$ mice and cultured without ($n = 5$) or with T_{regs} at 1:1 ratio from wild-type B6 ($n = 6$), $APC^{\Delta 468}$ ($n = 5$), or IL-$17^{-/-}$ BM in $APC^{\Delta 468}$ ($n = 6$), or with RORγ$t^{-/-}$x$APC^{\Delta 468}$ ($n = 5$) mice. (**B**) Compiled values of percent MC degranulation sensitized (IgE) and cross-linked with anti-IgE (IgE + Ag) and incubated without ($n = 10$) or with T_{regs} from wild-type B6 ($n = 16$), $APC^{\Delta 468}$ ($n = 15$), IL-$17^{-/-}$ BM in $APC^{\Delta 468}$ ($n = 8$), or RORγ$t^{-/-}$x$APC^{\Delta 468}$ ($n = 10$) mice. (**C**) Frequency of polyps after retro-orbital adoptive transfer of 5×10^5 T_{regs} into 2.5-month-old $APC^{\Delta 468}$ mice. Polyp number was determined 3 weeks later. B6 ($n = 5$), $APC^{\Delta 468}$ ($n = 4$), RORγ$t^{-/-}$x$APC^{\Delta 468}$ ($n = 3$). (**D**) Representative dot plot of intracellular cytokines in T_{regs} derived from the spleen of wild-type B6 or RORγ$t^{-/-}$ mice. Purified T_{regs} were cultured without or with MCs for 5 days in the presence of IL-2 and stem cell factor (SCF). Cells were gated on live $CD4^+CD25^+Foxp3^+$ cells ($n = 3$). Statistics are found in table S7.

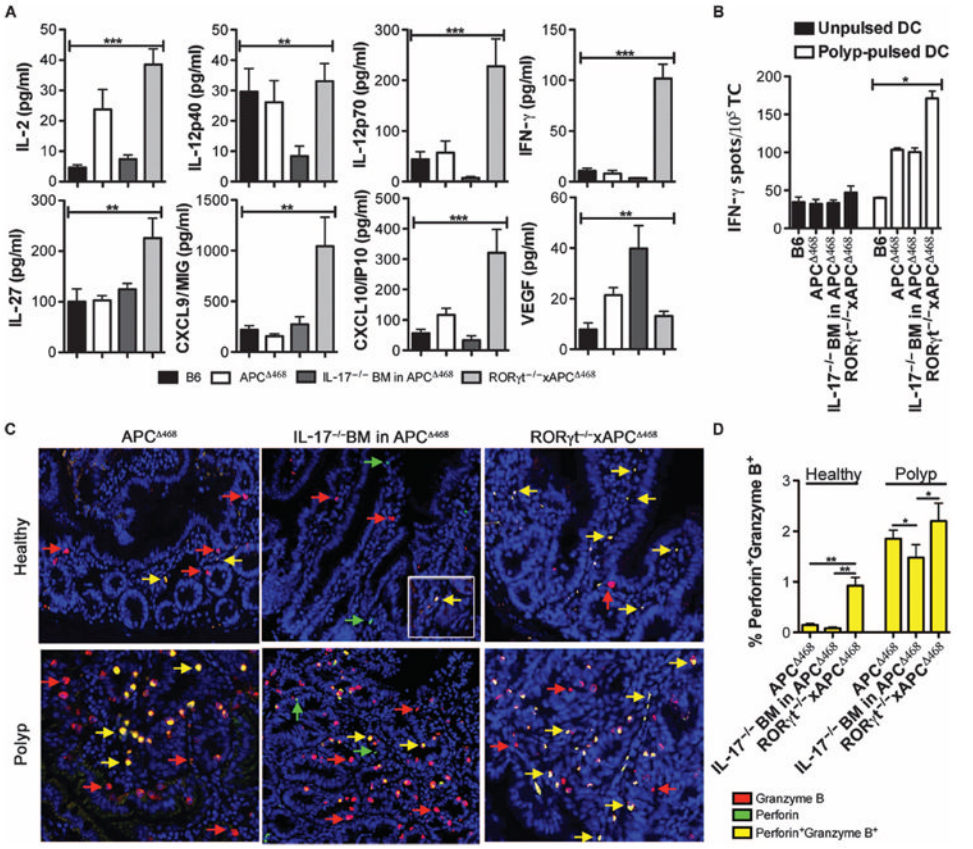

Fig. 8.

Protective inflammation and antitumor immunity is enhanced upon loss of RORγt in polyp-prone mice. (**A**) Amount of serum cytokines and chemokines from wild-type B6, APC$^{\Delta 468}$, IL-17$^{-/-}$BM in APC$^{\Delta 468}$, and RORγt$^{-/-}$xAPC$^{\Delta 468}$ mice as determined by multiplex ELISA. Sera from five mice were each tested in duplicate. (**B**) Improved polyp-specific T cell response assayed by IFN-γ ELISPOT. B6 dendritic cells (DCs) were pulsed with polyp lysate from APC$^{\Delta 468}$ mice as a source of tumor-associated antigens. Loaded DCs were then used to stimulate spleen-derived CD3^{+} T cells of either APC$^{\Delta 468}$, IL-17$^{-/-}$ BM in APC$^{\Delta 468}$, or RORγt$^{-/-}$xAPC$^{\Delta 468}$ mice. T cells from wild-type B6 spleen were used as a control. T cells were also tested on unpulsed DCs to verify that the response was tumor antigen–specific. Black bars, unpulsed DCs; white bars, pulsed DCs. (**C**) Representative immunofluorescence images of paraffin-embedded sections from APC$^{\Delta 468}$, APC$^{\Delta 468}$ reconstituted with IL-17$^{-/-}$ BM, or RORγt$^{-/-}$xAPC$^{\Delta 468}$ mice stained for perforin (red), granzyme B (green), and 4’,6-diamidino-2-phenylindole (DAPI) (blue); yellow arrow depicts granzyme B^{+}perforin^{+} cells. Double-positive cells in healthy tissue of IL-17$^{-/-}$ BM APC$^{\Delta 468}$ are rare, but inset depicts that they are present. (**D**) Compiled frequencies of granzyme B^{+}perforin^{+} cells (yellow) among total cells within a 200× field of view; $n = 3$ mice. Mean and SEM are depicted. Statistics are found in table S8.